Available online at www.sciencedirect.com
ScienceDirect
Scripta Materialia 63 (2010) 613–616
Scripta MATERIALIA
www.elsevier.com/locate/scriptamat

Grain size and reversible beta-to-omega phase transformation in a Ti alloy

Y.B. Wang,[a] Y.H. Zhao,[b] Q. Lian,[a] X.Z. Liao,[a,*] R.Z. Valiev,[c] S.P. Ringer,[d] Y.T. Zhu[e] and E.J. Lavernia[b]

[a] *School of Aerospace, Mechanical and Mechatronic Engineering, The University of Sydney, NSW 2006, Australia*
[b] *Department of Chemical Engineering and Materials Science, University of California at Davis, Davis, CA 95616, USA*
[c] *Institute of Physics of Advanced Materials, Ufa State Aviation Technical University, K. Marksa 12, Ufa 450000, Russia*
[d] *Australian Centre for Microscopy and Microanalysis, The University of Sydney, NSW 2006, Australia*
[e] *Department of Materials Science and Engineering, North Carolina State University, Raleigh, NC 27695-7919, USA*

Received 23 April 2010; revised 28 May 2010; accepted 28 May 2010
Available online 1 June 2010

We report a significant grain size effect on the phase transformation in a Ti–36Nb–2.2Ta–3.7Zr–0.3O alloy during severe plastic deformation. For grain sizes larger than the submicrometer range, the body-centered cubic β phase transformed to hexagonal ω phase when deformed by high-pressure torsion under a relatively low pressure of 3 GPa and at room temperature. However, a reverse ω to β transformation was observed under the same deformation conditions when the grain sizes were less than 100 nm.

Keywords: Titanium alloy; Severe plastic deformation; Phase transformation; Nanocrystalline

Reducing the grain sizes of materials to the nanocrystalline (nc, <100 nm) regime changes significantly the physical, chemical and mechanical behavior of the materials [1,2]. For example, under a low strain rate at room temperature, nc metallic materials with medium to high stacking fault energies deform via partial dislocation emission from grain boundaries (GBs) for grains of a few tens nanometers [3–5] or via grain rotation for grains of ~10 nm [6,7], while their coarse-grained counterparts usually deform via perfect dislocation activities. Nanoscale grain size also has a significant impact on phases and phase transformation [8–11]. For example, the stable structure of Co particles prepared by sputter deposition has been shown to vary with grain size and the martensitic transformation in shape-memory Ni–Ti alloys is completely suppressed when the grain size is <60 nm. The order–disorder transformation temperature of a Co–Pt alloy with grain sizes of ~3 nm was reported to be 175–325 °C lower than that of the coarse-grained equivalent.

Deformation-induced phase transformations are common in Ti alloys. For example, the reversible shape memory transformation between orthorhombic α″ phase and body-centered cubic β phase has been widely investigated [12–15]. Stress-induced phase transformation from β phase to the metastable hexagonal ω phase was observed in Ti alloys [16–19]. A reverse ω to β transformation has also been reported, but was only observed under very high pressure of ~140 GPa or high temperature [16,20].

In this paper, we report new observations of a striking grain size effect on the deformation-induced phase transformation in a Ti–36Nb–2.2Ta–3.7Zr–0.3O (at.%) alloy. The β to ω phase transformation occurred during the initial stages of high-pressure torsion (HPT) processing of the alloy under a relatively low pressure of 3 GPa at room temperature. However, the reverse transformation occurred during the same HPT process when the grain sizes were reduced to the nc regime, indicating that large grain sizes promote the β to ω forward phase transformation, while nanoscale grain sizes drive the reverse phase transformation.

An ingot of the Ti alloy was produced by arc melting and extruded into a long round bar at 1010 °C. Disks of around 1.7 mm thick and 20 mm in diameter were sectioned from the extruded bar and deformed using HPT for 1/4, 1/2, 1 and 5 turns, respectively, under

* Corresponding author. Tel.: +61 2 9351 2348; fax: +61 2 9351 7060; e-mail: xiaozhou.liao@sydney.edu.au

1359-6462/$ - see front matter © 2010 Acta Materialia Inc. Published by Elsevier Ltd. All rights reserved.
doi:10.1016/j.scriptamat.2010.05.045

3 GPa and a strain rate of 10^{-1} s^{-1} at room temperature. Transmission electron microscopy (TEM) specimens were sampled from the as-received material and from the center to the edge of each HPT disk. TEM observations were carried out using a JEOL 3000F operating at 300 kV. The average grain sizes were determined directly from TEM images by counting at least 100 randomly selected grains in each of those strain states. Dislocation densities and the area fraction of the ω phase were estimated from high-resolution TEM (HRTEM) images. Note that it is very difficult to estimate the volume fraction of the ω phase as the thickness of each ω particle along the electron beam direction is unknown. Therefore, we use the area fraction to qualitatively represent the amount of the ω phase in the material. The von Mises equivalent strains were calculated using the equation $\varepsilon = \frac{2\pi Nr}{\sqrt{3}h}$, where r is the distance from the disk centre, h is the thickness of the disk and N is the number of HPT turns. Hardness measurements were carried out using a Leco LV700AT hardness tester under a load of 10 kg with a 15 s dwell time. The hardness values were collected along seven radial directions on an HPT disk. Eight points were measured along each radial direction at an interval of 1 mm and values for each radius/strain value were averaged from the seven datum points.

Extensive TEM investigations revealed that the as-received material comprised of two phases: the β phase matrix and a small amount of the ω phase distributed uniformly throughout the β matrix (see Fig. 1). The average grain size of the matrix phase is about 2 μm. A typical TEM image of the β phase matrix is provided in Figure 1a with the inset selected-area electron diffraction (SAED) pattern obtained from a $<1\ 1\ 0>_\beta$ zone axis. Very weak diffuse diffraction spots located at 1/3 and 2/3 $\{1\ 1\ 2\}_\beta$ are from the ω phase. Figure 1b shows a HRTEM image recorded along a $<1\ 1\ 0>_\beta$ zone axis. The black and white ellipses in Figure 1b indicate the size, shape and locations of the ω phase presented in the β matrix. Note that because of the structural similarity and coherent nature of the interface between the β and ω phases, no sharp boundary is seen between them. The ellipses in Figure 1b (and Fig. 2b below) are approximate indications of the phase boundaries. The ω phase particles were 3–5 nm long along $<1\ 1\ 1>_\beta$ and 2–4 nm wide and their area fraction is about 7%. The structure of the ω phase within the β matrix is more clearly seen in a magnified image of the black ellipse (Fig. 1c). Atomic planes and directions in Figure 1c were indexed by noting that the incident electron beam was parallel to the $[0\bar{1}1]_\beta$ and the $[1\bar{2}10]_\omega$. Four white spots and four black spots represent the structural feature of the ω phase and the β phase, respectively. The interplanar distances of 0.28 and 0.40 nm for the $(0\ 0\ 0\ 1)_\omega$ and $(\bar{1}\ 0\ 1\ 0)_\omega$ planes, respectively, are indicated in Figure 1c. The orientation relationship between the ω and the β phase was thus deduced as $\{\bar{1}010\}_\omega//\{211\}_\beta$ $[0\ 0\ 0\ 1]_\omega//<1\ 1\ 1>_\beta$ and $<1\bar{2}10>_\omega//<0\ 1\ 1>_\beta$, which is consistent with the well-established orientation relationship between these two phases in Ti- and Zr-based alloys [17,20].

A significant increase in the volume fraction of the ω phase was observed after the commencement of HPT processing. Figure 2a shows a TEM image near the central area of the 1/4 turn HPT disk, where the strain is ~0.5. The average grain size of the matrix remained ~2 μm. However, strain contrast, in the form of blurred black-and-white stripes, was apparent within grains. The

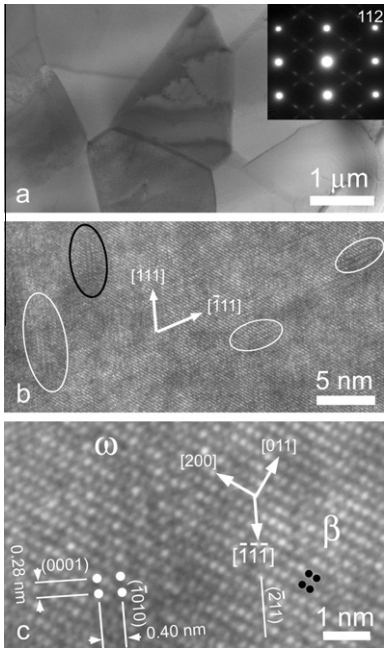

Figure 1. (a) A bright-field TEM image and an SAED pattern for the as-received Ti alloy; (b) a HRTEM image along $[0\bar{1}1]_\beta$ with ω phase particles highlighted by black and white ellipses; (c) an enlarged image surrounding the black elliptical area in (b). The structural feature of the ω phase and the β phase are marked by four white dots and four black dots, respectively. Atomic planes and directions are indexed.

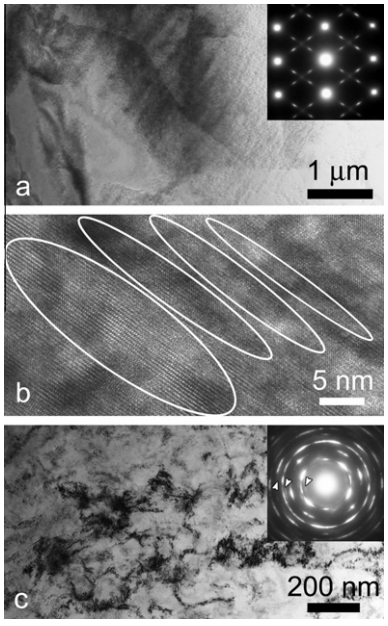

Figure 2. (a) A bright-field image and an SAED pattern taken near the central part of the 1/4 turn HPT disk (strain value = ~0.5); (b) an HRTEM image with ω phase particles marked by ellipses; (c) a bright-field image and an inset SAED pattern taken from the edge of the 1/4 turn HPT disk (strain value = ~4). Arrows in the SAED pattern indicate diffraction rings from solely the ω phase.

inset SAED pattern in Figure 2a, which was obtained by using the same experimental conditions (aperture size, electron beam intensity and exposure time) as that inset in Figure 1a, reveals that the intensity of the diffraction spots from the ω phase is much stronger than that in Figure 1a, further indicating that the volume fraction of the ω phase has increased significantly and confirming that a β to ω transformation occurred during deformation. Figure 2b shows a typical HRTEM image confirming a high density of the ω phase distributed in the β matrix and a length increase of the ω phase grains to ~40 nm. The estimated area fraction reached 24%.

Investigation of the edge part of the 1/4 turn HPT disk suggested that increasing strain (to ~4) resulted in an increase in the area fraction of the ω phase from ~24% to ~37% while at the same time grain sizes were reduced because of the HPT-induced grain refinement. Figure 2c shows a typical TEM image at the edge of the 1/4 turn disk, in which the average grain size was ~190 nm. Inset in Figure 2c is an SAED pattern with diffraction rings from the ω phase indicated by arrows. This result suggests that the ω phase still existed in the ultrafine-grained areas of the HPT disk.

Further increasing the strain values reduced grain sizes down to the nc regime and resulted in the disappearance of the ω phase. Figure 3a shows a typical TEM image of the 1 turn HPT disk, where the strain value at the edge of the disk is >15. A homogeneous structure with randomly oriented nc grains of ~50 nm was seen throughout the 1 turn HPT disk. A typical SAED pattern from the disk is inserted in Figure 3a, presenting diffraction rings only from the β phase. A typical HRTEM image from the disk is shown in Figure 3b, which further confirms that the β phase is the only existing phase when grain sizes are in the nc regime. Black dashed lines are used to mark grain boundaries in Figure 3b, although the boundaries are not clearly defined. The approximate orientation of each grain is indexed in Figure 3b. It is worth mentioning that rapid grain refinement was achieved in this material and the average grain size in the 1 turn disk is very close to that of the 5 turn disk. The microstructures of both the 1 and 5 turn HPT disks are homogeneous.

TEM investigations of the 1/2 turn disk revealed the presence of transition regions in which ultrafine-grained areas and nc areas coexist when strain value is ~8. HRTEM images and SAED patterns obtained from these transition regions confirmed that a large amount of the ω phase was found in the ultrafine-grained areas but no ω phase was seen in the nc areas. Statistic analysis of the HRTEM images from the 1/2 turn disk shows that the average length of ω particles is ~30 nm and their area fraction decreased to ~16%.

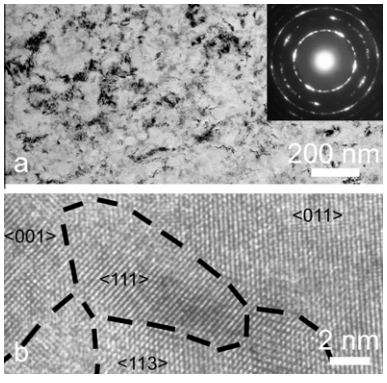

Figure 3. (a) A bright-field image and an SAED pattern; (b) an HRTEM image taken from the 1 turn HPT disk (strain value = ~15). Grain orientations are indexed. Grain boundaries are highlighted using dash lines.

To ensure these observations were systematic and not merely an artifact of a non-uniform distribution of phases, extensive TEM observations over a large range of specimens and areas were carried out. The results were systematic and confirmed that the phenomena reported above are universal for the Ti alloy investigated here. The above-mentioned experimental results are summarized in Table 1, which also includes data of dislocation density and hardness that are discussed below.

The experimental results indicate that the β to ω transformation occurred at the initial stages of HPT when grain sizes were relatively large. This transformation has contributed significantly to the initial rapid grain refinement down to the ultrafine-grained region. The mechanism of this β to ω transformation has been well documented [16]. However, with increasing strain values, grain sizes were reduced to the nc regime and the reverse ω to β transformation occurred until the ω phase disappeared completely.

There are two possible scenarios for the above experimental results: (1) the grain refinement down to nc region was caused by the reverse ω to β transformation (hereafter referred to as scenario I); and (2) nc grains caused the ω to β transformation (scenario II). For scenario I, we would expect to find that some {2 1 1} planes from neighboring nc β phase grains have 120° misorientation if these grains were transformed from the same ω phase grains because of the orientation relationship of $\{\bar{1}010\}_{\omega}//\{2\,1\,1\}_{\beta}$ mentioned before and because of the 120° orientation difference between different $\{\bar{1}010\}_{\omega}$ planes. Extensive survey of nc β phase grains in the 1 turn HPT disk found that this kind of orientation relationship was rare among neighboring nc β phase grains. We would also expect to see a gradual reduction of the amount of the ω phase during the reverse ω to β phase transformation for scenario I and some remnant ω particles should also be seen in nc grains. However, the immediate disappearance of the ω phase was seen in nc areas even though a large amount of the ω phase was found in neighboring ultrafine-grained areas in the 1/2 turn disk. In other words, our results do not support scenario I.

Our analysis of data supports scenario II, as is now discussed. Phase transformation pathways are known to be affected by the microstructure and applied stress. The dislocation density and the hardness presented in Table 1 showed no significant change immediately before and after the change of the phase transformation direction, and therefore are not the cause of the observed reverse transformations. The only significant and systematic change is the grain size (from 190 to 50 nm). In other words, it appears that the nc grains are responsible for the reverse (ω to β transformation. This observation is similar to the reported change in deformation mechanisms in nc metals [3–7]. This is the first observation of reverse phase transformation caused by nc grains.

Table 1. Summary of phase transformation, microstructure and hardness at different HPT strain values.

Sample position	As-received	1/4-turn centre	1/4-turn edge	1/2-turn edge	1-turn edge
von Mises strain	0	~0.5	~4	~8	~15
Transition	N/A	$\beta \rightarrow \omega$	$\beta \rightarrow \omega$	$\beta \leftrightarrow \omega$	$\omega \rightarrow \beta$
Phase/s present	$\beta + \omega$	$\beta + \omega$	$\beta + \omega$	$\beta + \omega$	β
Area fraction of ω	7%	24%	37%	16%	0%
ω Particle length	4 nm	40 nm	60 nm	30 nm	0
Average grain size	1.8 μm	1.8 μm	190 nm	80 nm	50 nm
Dislocation density $\times 10^{16}$ m^{-2}	2.2	4.5	6.5	6.2	5.7
Hv	260 ± 5.2	280 ± 5.7	296 ± 4.8	294 ± 5.0	290 ± 5.3

The ω to β transformation usually occurs under high pressures (e.g. 30 GPa for Zr, 71 GPa for Hf and 140 GPa for Ti metal) [21]. The results presented in this paper show that this transformation can occur at a relatively low pressure of 3 GPa. Shear deformation could help with reducing the pressure needed for some transformations. For example, the $\alpha \rightarrow \omega + \beta$ transformation in Zr usually occurs under a pressure of 30 GPa [20,21], but the pressure needed for the transformation was significantly reduced to 3 GPa when the material was processed using HPT [22]. First-principles calculations showed that the pressure needed for certain pressure-induced martensitic transformations decreases with increasing shear [23]. However, in the present study, the HPT parameters, including pressure and strain rate, were kept constant, suggesting that a factor other than processing condition has caused the transformation to proceed first forward and later backward. This further supports scenario II, i.e. nc grains caused the reverse phase transformation.

In summary, β to ω and ω to β phase transformations were observed at different stages of a single HPT process of a Ti–36Nb–2.2Ta–3.7Zr–0.3O alloy. It appears that the reverse (ω to β) phase transformation was caused primarily by nc grain size. These observations are another example of the unexpected behavior of nanocrystalline materials.

The authors are grateful for scientific and technical input and support from the Australian Microscopy and Microanalysis Research Facility node at the University of Sydney. This project is supported by the Australian Research Council (Grant no. DP0772880 (Y.B.W., Q.L. and X.Z.L.)), the Office of Naval Research (Grant no. N00014-08-1-0405 (Y.H.Z. and E.J.L.)), and the US Army Research Office and Army Research Laboratory (Y.T.Z.).

[1] H. Gleiter, Acta Mater. 48 (2008) 1.
[2] M.A. Meyers, A. Mishra, D.J. Benson, Prog. Mater. Sci. 51 (2006) 427.
[3] X.Z. Liao, F. Zhou, E.J. Lavernia, S.G. Srinivasan, M.I. Baskes, D.W. He, Y.T. Zhu, Appl. Phys. Lett. 83 (2003) 632.
[4] X.Z. Liao, Y.H. Zhao, S.G. Srinivasan, Y.T. Zhu, R.Z. Valiev, D.V. Gunderov, Appl. Phys. Lett. 84 (2004) 592.
[5] V. Yamakov, D. Wolf, S.R. Phillpot, A.K. Mukherjee, H. Gleiter, Nat. Mater. 1 (2002) 45.
[6] Z.W. Shan, E.A. Stach, J.M.K. Wiezorek, J.A. Knapp, D.M. Follstaedt, S.X. Mao, Science 305 (2004) 654.
[7] Y.B. Wang, J.C. Ho, X.Z. Liao, H.Q. Li, S.P. Ringer, Y.T. Zhu, Appl. Phys. Lett. 94 (2009) 011908.
[8] O. Kitakami, H. Sato, Y. Shimada, Phys. Rev. B 56 (1997) 13849.
[9] Y. Ivanisenko, I. MacLaren, X. Sauvage, R.Z. Valiev, H.J. Fecht, Acta Mater. 54 (2006) 1659.
[10] T. Waitz, V. Kazykhanov, H.P. Karnthaler, Acta Mater. 52 (2004) 137.
[11] D. Alloyeau, C. Ricolleau, C. Mottet, T. Oikawa, C. Langlois, Y. Le Bouar, N. Braidy, A. Loiseau, Nat. Mater. 8 (2009) 940.
[12] Y.L. Hao, S.J. Li, S.Y. Sun, C.Y. Zheng, Q.M. Hu, R. Yang, Appl. Phys. Lett. 87 (2005) 091906.
[13] W. Xu, K.B. Kim, J. Das, M. Calin, B. Rellinghaus, J. Eckert, Appl. Phys. Lett. 89 (2006) 031906.
[14] D.H. Ping, Y.Y. Mitarai, C.Y. Cui, F.X. Yin, M.A. Choudhry, Appl. Phys. Lett. 93 (2008) 151911.
[15] J.P. Cui, Y.L. Hao, S.J. Li, M.L. Sui, D.X. Li, R. Yang, Phys. Rev. Lett. 102 (2009) 045503.
[16] S.K. Sikka, Y.K. Vohra, R. Chidambaram, Prog. Mater. Sci. 27 (1982) 245.
[17] R.J. Talling, R.J. Dashwood, M. Jackson, D. Dye, Acta Mater. 57 (2009) 1188.
[18] H. Xing, J. Sun, Appl. Phys. Lett. 93 (2008) 031908.
[19] Y. Yang, G.P. Li, G.M. Cheng, Y.L. Li, K. Yang, Appl. Phys. Lett. 94 (2009) 061901.
[20] G.K. Dey, R. Tewari, S. Banerjee, G. Jyoti, S.C. Gupta, K.D. Joshi, S.K. Sikka, Acta Mater. 52 (2004) 5243.
[21] H. Xia, S.J. Duclos, A.L. Ruoff, Y.K. Vohra, Phys. Rev. Lett. 64 (1990) 204.
[22] M.T. Pérez-Prado, A.P. Zhilyaev, Phys. Rev. Lett. 102 (2009) 175504.
[23] K.J. Caspersen, A. Lew, M. Ortiz, E.A. Carter, Phys. Rev. Lett. 93 (2004) 115501.